

## A New Nadarajah-Haghighi Generalization with Five Different Shapes for the Hazard Function

Una nueva generalización de la distribución Nadarajah-Haghighi con cinco formas diferentes de función de hazard

FERNANDO A. PEÑA-RAMÍREZ<sup>1,a</sup>, RENATA ROJAS GUERRA<sup>2,b</sup>,  
GAUSS M. CORDEIRO<sup>3,c</sup>

<sup>1</sup>DEPARTMENT OF STATISTICS, FACULTAD DE CIENCIAS, UNIVERSIDAD NACIONAL DE COLOMBIA, BOGOTÁ, COLOMBIA

<sup>2</sup>DEPARTMENT OF STATISTICS, CENTRO DE CIÊNCIAS NATURAIS E EXATAS, UNIVERSIDADE FEDERAL DE SANTA MARIA, SANTA MARIA, BRASIL

<sup>3</sup>DEPARTMENT OF STATISTICS, CENTRO DE CIÊNCIAS EXATAS E DA NATUREZA, UNIVERSIDADE FEDERAL DE PERNAMBUCO, RECIFE, BRASIL

---

### Abstract

We introduce a four-parameter model called the Weibull Nadarajah-Haghighi distribution. It is obtained by inserting the Nadarajah-Haghighi distribution in the Weibull-G family. The proposed distribution can produce constant, increasing, decreasing, bathtub, and upside down-bathtub hazard rate shapes, which are the most important in lifetime analysis. We explore some structural properties, including the quantile function, ordinary and incomplete moments, mean deviations, Bonferroni and Lorenz curves, and Rényi entropy. The maximum likelihood method is used to estimate the model parameters. A simulation study is formed to examine the precision of the estimates. The usefulness of the new distribution is illustrated through two applications to real data. The new model provides better fits than some widely known lifetime distributions.

**Key words:** Hazard rate function; Lifetime data; Maximum likelihood; Nadarajah-Haghighi distribution; Weibull-G family.

### Resumen

Este trabajo introduce un nuevo modelo probabilístico de cuatro parámetros llamado distribución Weibull Nadarajah-Haghighi. Este modelo es obtenido mediante la inserción de la distribución Nadarajah-Haghighi en la

---

<sup>a</sup>Assistant Professor. E-mail: fapenara@unal.edu.co

<sup>b</sup>Assistant Professor. E-mail: renata.r.guerra@ufsm.br

<sup>c</sup>Full Professor. E-mail: gauss@de.ufpe.br

familia Weibull-G. Un punto destacado de esta nueva propuesta son sus formas en la función de hazard: constante, creciente, decreciente, bañera y bañera invertida, que son las más importantes en el análisis de supervivencia. En este trabajo también se exploran algunas propiedades estructurales del modelo, como la función cuantil, los momentos ordinarios e incompletos, las desviaciones medias, las curvas de Bonferroni y Lorenz y la entropía de Rényi. Para la estimación de los parámetros, se utiliza el método de máxima verosimilitud. Además, un estudio de simulación de Monte Carlo se realiza para examinar el desempeño de las estimaciones. La utilidad de la nueva distribución se ilustra a través del ajuste en dos conjuntos de datos reales. El nuevo modelo muestra mejores ajustes que algunas distribuciones consideradas canónicas en análisis de supervivencia.

**Palabras clave:** Distribución Nadarajah-Haghighi; Familia Weibull-G; Función de hazard; Máxima verosimilitud; Tiempos de sobrevida.

## 1. Introduction

The Nadarajah-Haghighi (NH) distribution was introduced by [Nadarajah & Haghighi \(2011\)](#) for modeling zero-mode data. It has mainly been applied in survival analysis and reliability estimation ([Almarashi et al., 2022](#); [Elshahhat et al., 2022](#)). In this context, the NH model is considered an alternative to the gamma, Weibull, and exponentiated-exponential distributions since it presents a decreasing shape for its probability density function (pdf) and allows increasing, constant, or decreasing shapes for the hazard rate function (hrf). Although, it is not appropriate for bathtub and upside-down bathtub-shaped (or unimodal) hazard rates.

Such failure rates are appeared when analyzing complex electronic and mechanical systems. For example, upside-down bathtub hazard rates can be encountered in repairable systems ([Louzada et al., 2018](#)), reliability-centered maintenance ([Ramos et al., 2018](#)), and fatigue failures ([Jiang et al., 2003](#)). In contrast, the bathtub shape are common in the reliability of embedded software in hardware devices ([Singla et al., 2012](#)), and wind turbines ([Pérez et al., 2013](#)) among others. Readers are referred to [Klutke et al. \(2003\)](#) for a detailed discussion on the occurrence of bathtub shape failures.

Due to the relevance of these features, several authors proposed generalizations of the NH distribution. For example, [Lemonte \(2013\)](#) pioneered the exponentiated Nadarajah-Haghighi (ENH), [Bourguignon et al. \(2015\)](#) introduced the gamma Nadarajah-Haghighi (GNH) distribution. The NH model is also a special case of the power generalized Weibull (PGW) ([Bagdonavicius & Nikulin, 2002](#)), exponentiated power generalized Weibull ([Peña-Ramírez et al., 2018](#)), Nadarajah-Haghighi Lindley ([Peña-Ramírez et al., 2019](#)) and logistic Nadarajah-Haghighi ([Peña-Ramírez et al., 2020](#)) distributions. On the other hand, to the best of our knowledge, the Weibull generalized (Weibull-G) family ([Bourguignon et al., 2014](#)) have not been considered to derive a lifetime distribution from the NH distribution.

The Weibull-G family extends the Weibull distribution by applying its odds ratio and adding two extra parameters to furnish a more flexible distribution

(Bourguignon et al., 2014). Afterward, specific baselines have often been addressed to this family, thus allowing to obtain generalized models that accommodate different patterns for their densities and hazard rates (Oguntunde et al., 2015; Guerra et al., 2021). In this paper, we use this approach to propose a new four-parameter model called the Weibull Nadarajah-Haghighi (WNH) distribution. Our primary motivation is that new distribution allows for greater flexibility of its pdf than the baseline density. The WNH density can be unimodal and is quite flexible for skewness and kurtosis. In addition, it contains as particular models some well-known distributions such as the Weibull-Exponential (WExp) and the Gompertz distribution models.

Secondly, the WNH presents five different shapes for the hazard function, i.e., decreasing, increasing, upside-down bathtub, and bathtub-shaped forms. This feature makes the new distribution quite competitive with other popular lifetime models and very attractive to be used in reliability applications. As highlighted by Xu et al. (2017), using distributions that unify monotonic and non-monotonic hazard shapes is a flexible and elegant way to deal with failure data fitting. For example, the bathtub-shaped hrf is reproduced by the WNH distribution using a single set of four parameters for all the regions of the hazard function.

In practical situations, we note that the WNH distribution may provide better fits than other generated models under the NH baseline. See the results of Section 7. They reveal that the WNH model can be a valuable alternative to other NH-generated distributions and widely known lifetime models.

The paper is outlined as follows. Section 2 defines the new model and its theoretical background. In Section 3, we derive a linear representation for the WNH density function. In Section 4, a broad variety of its structural properties are explored. The estimation of the model parameters by maximum likelihood and using a Bayesian approach is presented in Section 5. A simulation study is performed in Section 6 to examine the adequacy of the maximum likelihood estimates (MLEs). Section 7 provides empirical applications for illustrative purposes. Section 8 offers some concluding remarks.

## 2. The Weibull Nadarajah-Haghighi distribution

The derivation of generalized distributions by adding parameters to an existing model is an instrumental technique in the statistical literature (Oluyede & Liyanage, 2023). These generalized models have been proposed to obtain flexible models, which can accommodate different configurations of skewness and non-monotonic shapes for the hrf (Marinho et al., 2018). We can cite Silva et al. (2019) and Peter et al. (2021) as some recent advances in the distribution theory.

In this context, Bourguignon et al. (2014) pioneered a family of univariate distributions generated by extending the Weibull model applied to the odds ratio. Let  $G(x)$  and  $g(x)$  denote the cumulative distribution function (cdf) and pdf of a baseline model with parameter vector  $\xi$ . Consider the Weibull cdf  $F(x) = 1 - e^{-ax^b}$  (for  $x > 0$ ,  $a > 0$  and  $b > 0$ ). The Weibull-G family follows by replacing

the argument  $x$  with the baseline's odds,  $G(x)/\overline{G}(x)$ , in the Weibull cdf, where  $\overline{G}(x) = 1 - G(x)$ . Then, for  $x \in \mathcal{D} \subseteq \mathbb{R}$ , the cdf and pdf of the Weibull-G family are

$$F(x; \alpha, \beta, \boldsymbol{\xi}) = \int_0^{\frac{G(x; \boldsymbol{\xi})}{1 - G(x; \boldsymbol{\xi})}} a b t^{b-1} e^{-a t^b} dt = 1 - \exp \left\{ -a \left[ \frac{G(x; \boldsymbol{\xi})}{\overline{G}(x; \boldsymbol{\xi})} \right]^b \right\} \quad (1)$$

and

$$f(x; \alpha, \beta, \boldsymbol{\xi}) = a b g(x; \boldsymbol{\xi}) \frac{G(x; \boldsymbol{\xi})^{b-1}}{\overline{G}(x; \boldsymbol{\xi})^{b+1}} \exp \left\{ -a \left[ \frac{G(x; \boldsymbol{\xi})}{\overline{G}(x; \boldsymbol{\xi})} \right]^b \right\}, \quad (2)$$

respectively. If  $b = 1$ , we have the exponentiated-G (exp-G) family. Note that the Weibull-G family does not have as a special case the baseline G distribution. However, we can consider the distributions of this family as a compounding model between the Weibull and the baseline distributions (Tahir et al., 2016).

The WNH distribution is defined by inserting the NH cdf in Equation (1). The cdf and pdf of the NH distribution are given by

$$G(x) = 1 - \exp\{1 - (1 + \lambda x)^\alpha\}, \quad x > 0, \quad (3)$$

and

$$g(x) = \alpha \lambda (1 + \lambda x)^{\alpha-1} \exp\{1 - (1 + \lambda x)^\alpha\}, \quad (4)$$

respectively, where  $\lambda$  and  $\alpha$  are positive scale and shape parameters, respectively. The exponential distribution is a special case when  $\alpha = 1$ .

Thus, the cdf of the WNH distribution

$$F(x) = 1 - \exp \left\{ -a [\exp\{(1 + \lambda x)^\alpha - 1\} - 1]^b \right\}, \quad (5)$$

and the pdf has the form

$$f(x) = a b \alpha \lambda (1 + \lambda x)^{\alpha-1} [1 - \exp\{1 - (1 + \lambda x)^\alpha\}]^{b-1} \times \exp \left\{ -b [1 - (1 + \lambda x)^\alpha] - a [\exp\{(1 + \lambda x)^\alpha - 1\} - 1]^b \right\}, \quad (6)$$

where  $a, b > 0$  are two extra shape parameters from the Weibull-G family,  $\alpha > 0$  is a shape and  $\lambda > 0$  is a scale from the baseline model.

Hereafter,  $X \sim \text{WNH}(a, b, \alpha, \lambda)$  denotes a random variable with pdf (6). The WNH distribution contains as special models some known distributions. For  $\alpha = 1$ , it reduces to the Weibull-Exponential distribution introduced by Oguntunde et al. (2015). If  $b = 1$  and  $\alpha = 1$ , it becomes the Gompertz distribution. Figure 1 displays plots of the WNH pdf for some parameter values and reveals that it allows to fit left and right skewed data. More details about these measures can also be found in Section 4.2.

The hrf of  $X$  becomes

$$\tau(x) = a b \alpha \lambda (1 + \lambda x)^{\alpha-1} [1 - \exp\{1 - (1 + \lambda x)^\alpha\}]^{b-1} \times \exp \{-b [1 - (1 + \lambda x)^\alpha]\}.$$

Figure 2 reports plots of the hrf of  $X$  which has at least five different shapes. These characteristics give great flexibility to the model. For example, its decreasing hazard shape can help analyze lifetime data in which earlier failures are corrected or when the specimens improve over time (Peña-Ramírez et al., 2020). The bathtub shape makes it feasible for survival analysis problems such as the human mortality experience. It presents a high infant mortality rate which decreases rapidly to reach a low level for quite a few years before increases again (Silva et al., 2010).

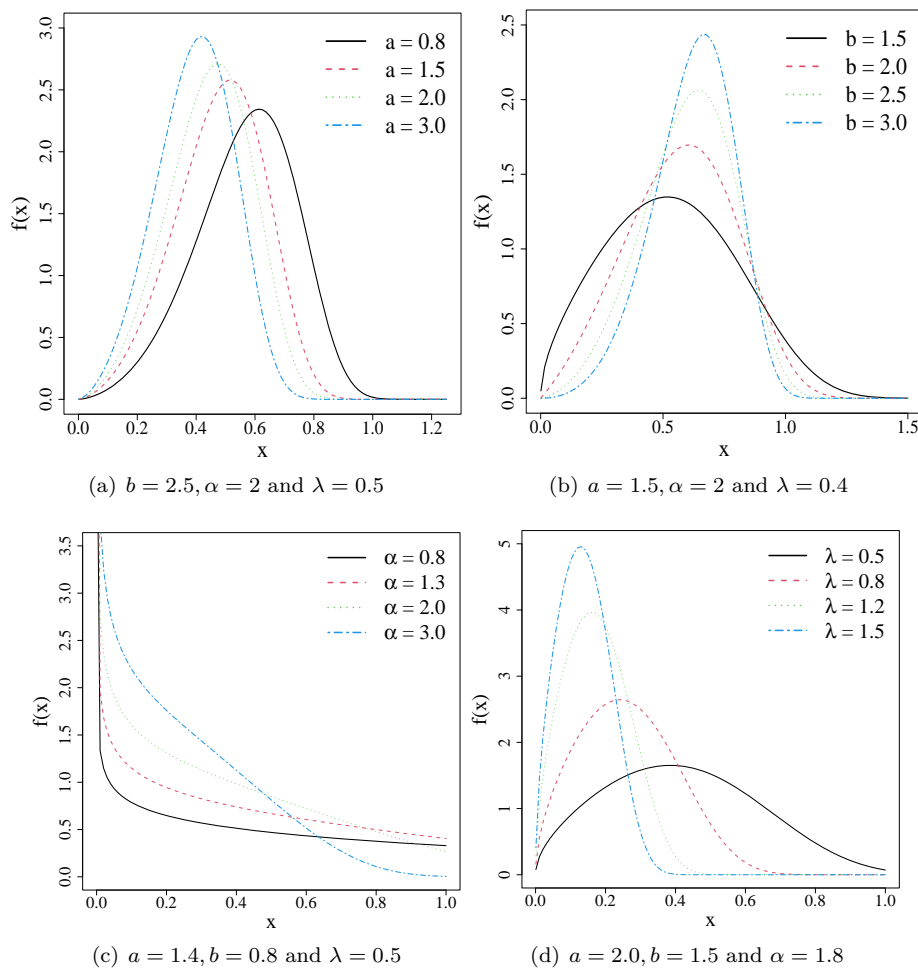


FIGURE 1: Plots of the WNH density.

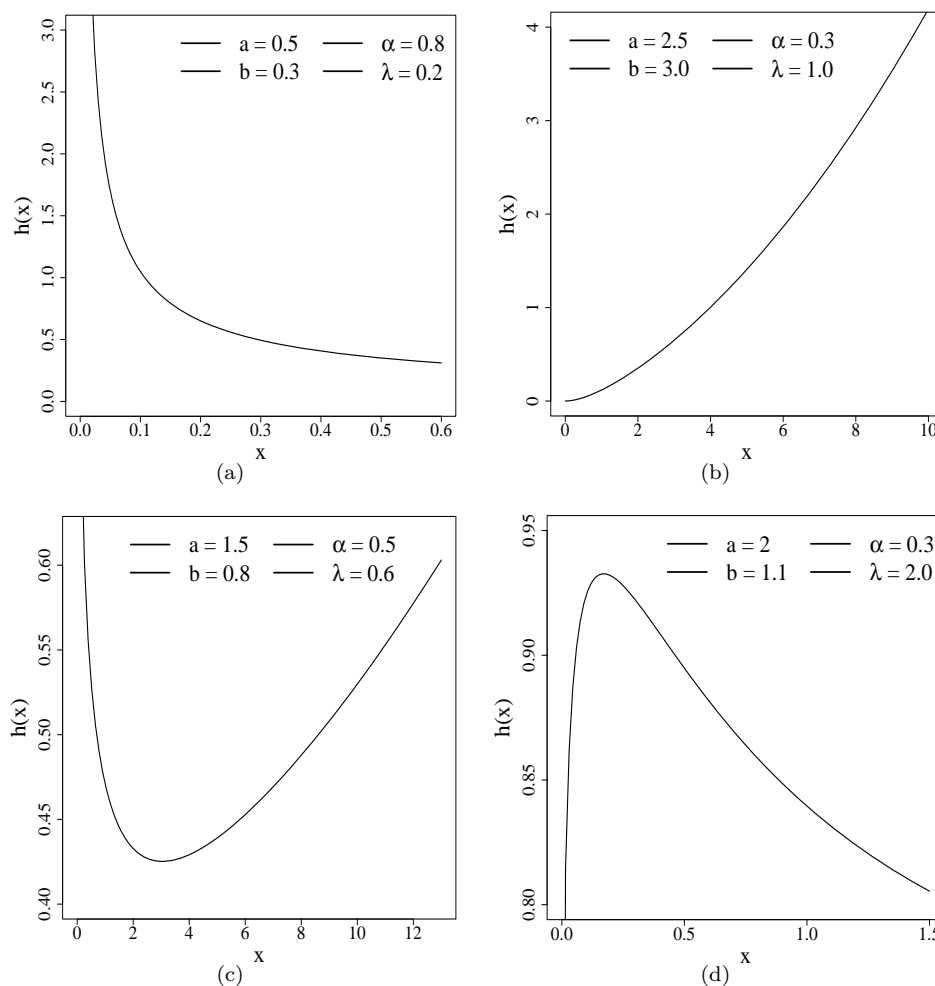


FIGURE 2: Plots of the WNH hrf.

### 3. Useful Expansion

Bourguignon et al. (2014) demonstrated that the Weibull-G pdf can be expressed in terms of the exp-G densities. Let  $G(y)$  be the baseline cdf of a random variable  $Y$ . The exp-G cdf is obtained by a power transformation  $H_c(y) = G(y)^c$  of  $G(y)$ , where  $c > 0$  is an additional shape parameter. Then, the exp-G density function is  $h_c(y) = c g(y) G(y)^{c-1}$ . Tahir & Nadarajah (2015) wrote a survey with other ways to obtain generated continuous distributions, and listed twenty-eight models using such a method. We can also refer to Peña-Ramírez et al. (2018) Martínez-Flórez et al. (2022) as recent advances in this family.

In this section, we derive a useful expansion for the WNH density based on the exp-G family. To this aim, we replace Equations (3) and (4) in (2), leading to

$$f(x) = a b \alpha \lambda (1 + \lambda x)^{\alpha-1} \exp\{1 - (1 + \lambda x)^\alpha\} \frac{[1 - \exp\{1 - (1 + \lambda x)^\alpha\}]^{b-1}}{[\exp\{1 - (1 + \lambda x)^\alpha\}]^{b+1}} \times \exp\left\{-a \left[\frac{1 - \exp\{1 - (1 + \lambda x)^\alpha\}}{\exp\{1 - (1 + \lambda x)^\alpha\}}\right]^b\right\}. \tag{7}$$

By expanding the exponential function in the last quantity in (7), we have

$$\exp\left\{-a \left[\frac{1 - \exp\{1 - (1 + \lambda x)^\alpha\}}{\exp\{1 - (1 + \lambda x)^\alpha\}}\right]^b\right\} = \sum_{i=0}^{\infty} \frac{(-1)^i a^i}{i!} \frac{[1 - \exp\{1 - (1 + \lambda x)^\alpha\}]^{ib}}{[\exp\{1 - (1 + \lambda x)^\alpha\}]^{ib}}.$$

Inserting the above expansion in (7) and after some algebra, we obtain

$$f(x) = a b \alpha \lambda (1 + \lambda x)^{\alpha-1} \exp\{1 - (1 + \lambda x)^\alpha\} \times \sum_{i=0}^{\infty} \frac{(-1)^i a^i}{i!} \frac{[1 - \exp\{1 - (1 + \lambda x)^\alpha\}]^{(i+1)b-1}}{[\exp\{1 - (1 + \lambda x)^\alpha\}]^{(i+1)b+1}}. \tag{8}$$

By using the generalized binomial theorem, we can rewrite the quantity  $[\exp\{1 - (1 + \lambda x)^\alpha\}]^{-[(i+1)b+1]}$  as

$$\{1 - [1 - \exp\{1 - (1 + \lambda x)^\alpha\}]\}^{-[(i+1)b+1]} = \sum_{j=0}^{\infty} \frac{\Gamma([i+1]b+j+1)}{j! \Gamma([i+1]b+1)} \times [1 - \exp\{1 - (1 + \lambda x)^\alpha\}]^j.$$

By inserting the last equation in (8) and after some simplifications, the WNH density function can be expressed as an infinite linear combination of exp-NH densities, namely

$$f(x) = \sum_{i,j=0}^{\infty} \omega_{i,j} h_{(i+1)b+j}(x), \tag{9}$$

where

$$\omega_{i,j} = \frac{(-1)^i b a^{i+1} \Gamma([i+1]b+j+1)}{i! j! [(i+1)b+j] \Gamma([i+1]b+1)}.$$

As mentioned before, the ENH model (Lemonte, 2013) is the exp-G distribution by taking for the baseline the NH model. Figure 3 reveals the convergence of  $S = \sum_{i,j=0}^n \omega_{i,j}$  for  $n = 1, 2, \dots, 15$  and  $a = b = 0.5$ . Equation (9) is the main result of this section.

## 4. Some Structural Properties

In this section, we obtain some structural properties of the WNH distribution from those of the ENH model. Our investigation includes the quantile function (qf), ordinary and incomplete moments, mean deviations, Bonferroni and Lorenz curves and Rényi entropy.

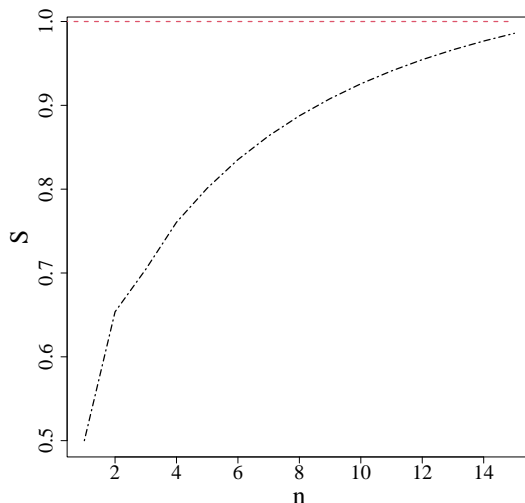


FIGURE 3: Sum of the coefficients  $S = \sum_{i,j=0}^n \omega_{i,j}$  of the linear combination in (9).

#### 4.1. Quantile Function

The qf of  $X$  is determined by inverting Equation (5). Thus, for  $u \in (0, 1)$ , we have

$$Q(u) = \frac{1}{\lambda} \left\{ \left[ 1 + \log \left( 1 + \left[ \frac{-\log(1-u)}{a} \right]^{\frac{1}{b}} \right) \right]^{\frac{1}{\alpha}} - 1 \right\}. \quad (10)$$

Setting  $u = 0.5$  gives the median  $M = Q(0.5)$  of  $X$ . The qf is a useful tool to obtain skewness and kurtosis measures and for simulating WNH random variable using the inverse transformation method. Let  $U$  be a standard uniform random variable. Thus, the random variable  $X = Q(U)$  has pdf given by (6).

#### 4.2. Ordinary and Central Moments

The  $s$ th ordinary moments of  $X$  follows from (9) as

$$\mu'_s = E(X^s) = \sum_{i,j=0}^{\infty} w_{i,j} \int_0^{\infty} x^s h_{(i+1)b+j}(x) dx.$$

Using a result in Lemonte (2013), we obtain

$$\begin{aligned} \mu'_s &= \lambda^{-s} \sum_{i,j,l=0}^{\infty} \sum_{k=0}^s \frac{(-1)^{s+l-k} [(i+1)b+j] e^{l+1} w_{i,j}}{(l+1)^{k/\alpha+1}} \\ &\quad \times \binom{(i+1)b+j-1}{l} \binom{s}{k} \Gamma\left(\frac{k}{\alpha} + 1, l+1\right), \end{aligned}$$



where  $\Gamma(a, x) = \int_x^\infty z^{a-1} e^{-z} dz$  denotes the complementary incomplete gamma function.

An alternative representation for the ordinary moments of  $X$  can be based on the NH qf. We can write

$$\mu'_s = \lambda^{-s} \sum_{i,j=0}^{\infty} w_{i,j} [(i+1)b + j] I_{i,j}^{(s)}(\alpha, b), \quad (11)$$

where  $I_{i,j}^{(s)}(\alpha, b) = \int_0^1 u^{(i+1)b+j-1} \{[1 - \log(1-u)]^{1/\alpha} - 1\}^s du$  can be evaluated numerically.

### 4.3. Skewness and Kurtosis

The Bowley skewness (Kenney & Keeping, 1962) and the Moors kurtosis (Moors, 1988) of  $X$  can also be defined in terms of the qf, respectively, by

$$B = \frac{Q(3/4) - 2Q(1/2) + Q(1/4)}{Q(3/4) - Q(1/4)},$$

and

$$M = \frac{Q(7/8) - Q(5/8) + Q(3/8) - Q(1/8)}{Q(3/4) - Q(1/4)},$$

where  $Q(\cdot)$  is given by (10).

Table 1 provides a numerical experiment that computes the first four moments,  $B$  and  $M$  coefficients for some parameter values of the WNH model. These scenarios are selected using the values from Figure 1. Thus, we can compare the measures with the density shapes. The results corroborate that the proposed distribution is quite flexible regarding the properties above. It can accommodate a wide range of values for the moments. For example,  $\mu'_1$  varies between 0.1416 (Scen. 16) and 1.2439 (Scen. 9). In contrast,  $\mu'_4$  has a variation between 0.0012 (Scen. 16) and 33.1512 (Scen. 9). For the skewness measure, note that  $B$  can have positive and negative values, thus indicating that the WNH distribution is useful for modeling left and right skewed data. For comparing Scen. 13 to 16, we note that  $\lambda$  does not affect  $B$  and  $M$ . This result is expected since  $\lambda$  is a scale parameter. Finally, Figure 4 reports contour lines of  $B$  and  $M$ , thus allowing a visual inspection of their behavior when varying  $a$  and  $b$ .

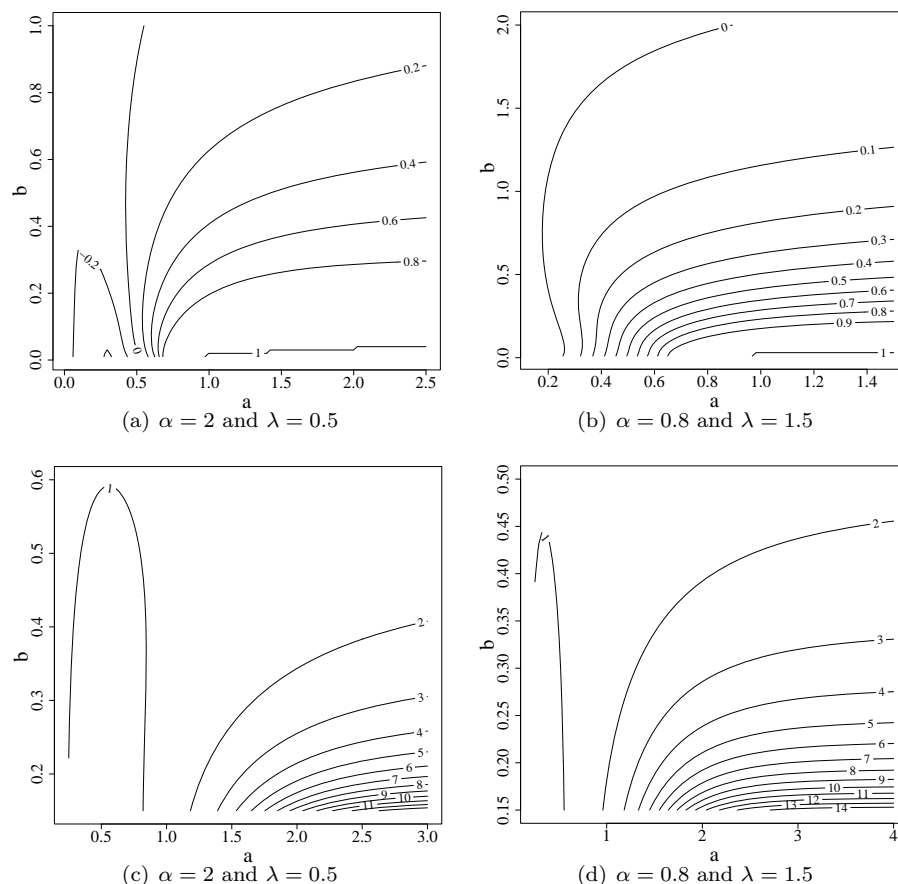


FIGURE 4: Contour lines of the WNH Bowley skewness ((a) and (b)) and Moors kurtosis ((c) and (d)).

### 4.4. Incomplete Moments and Mean Deviations

The incomplete moments provide high-value information in reliability and inequality studies. It is because they can be used to obtain the mean deviations and the Bonferroni and Lorenz curves. We derive those measures using the WNH distribution and provide a visual inspection of these curves for some selected scenarios.

Let  $m_s(y)$  denote the  $s$ th incomplete moment of  $X$ , say  $m_s(y) = \int_0^y x^s f(x)dx$ . From Equation (9), we can write

$$m_s(y) = E(X^s) = \sum_{i,j=0}^{\infty} w_{i,j} \int_0^y x^s h_{(i+1)b+j}(x) dx.$$

TABLE 1: First four moments,  $B$  and  $K$  for the WNH distribution.

Scen.	Parameter values				Statistical Properties					
	$a$	$b$	$\alpha$	$\lambda$	$\mu'_1$	$\mu'_2$	$\mu'_3$	$\mu'_4$	$B$	$M$
1	0.8	2.5	2.0	0.5	0.5680	0.3507	0.2295	0.1571	-0.0601	1.2170
2	1.5	2.5	2.0	0.5	0.4816	0.2544	0.1433	0.0848	-0.0490	1.2112
3	2.0	2.5	2.0	0.5	0.4450	0.2181	0.1143	0.0631	-0.0439	1.2090
4	3.0	2.5	2.0	0.5	0.3966	0.1742	0.0822	0.0409	-0.0369	1.2062
5	1.5	1.5	2.0	0.4	0.5391	0.3609	0.2744	0.2279	0.0129	1.1636
6	1.5	2.0	2.0	0.4	0.5754	0.3792	0.2730	0.2098	-0.0272	1.1924
7	1.5	2.5	2.0	0.4	0.6020	0.3975	0.2799	0.2071	-0.0490	1.2112
8	1.5	3.0	2.0	0.4	0.6220	0.4136	0.2888	0.2096	-0.0626	1.2239
9	1.4	0.8	0.8	0.5	1.2439	2.8886	8.9484	33.1512	0.2426	1.1984
10	1.4	0.8	1.3	0.5	0.6573	0.7463	1.0826	1.8242	0.1964	1.1430
11	1.4	0.8	2.0	0.5	0.3943	0.2586	0.2121	0.1993	0.1702	1.1161
12	1.4	0.8	3.0	0.5	0.2506	0.1022	0.0515	0.0295	0.1538	1.1010
13	2.0	1.5	1.8	0.5	0.4247	0.2279	0.1404	0.0952	0.0297	1.1640
14	2.0	1.5	1.8	0.8	0.2655	0.0890	0.0343	0.0145	0.0297	1.1640
15	2.0	1.5	1.8	1.2	0.1770	0.0396	0.0102	0.0029	0.0297	1.1640
16	2.0	1.5	1.8	1.5	0.1416	0.0253	0.0052	0.0012	0.0297	1.1640

We can show that  $m_s(y)$  is given by

$$m_s(y) = \lambda^{-s} \sum_{i,j=0}^{\infty} w_{i,j} [(i+1)b + j] \times \int_0^{1-e^{1-(1+\lambda y)^\alpha}} \{[1 - \log(1-u)]^{1/\alpha} - 1\}^s u^{(i+1)b+j-1} du.$$

Alternatively,

$$m_s(y) = \lambda^{-s} \sum_{i,j,l=0}^{\infty} \sum_{k=0}^s \frac{(-1)^{s+l-k} [(i+1)b + j] e^{l+1} w_{i,j} \binom{(i+1)b + j - 1}{l} \binom{s}{k}}{(l+1)^{k/\alpha+1}} \times \left[ \Gamma\left(\frac{k}{\alpha} + 1, l+1\right) - \Gamma\left(\frac{k}{\alpha} + 1, (l+1)(1+\lambda y)^\alpha\right) \right]. \tag{12}$$

The mean deviations about the mean and the median are given by  $\delta_1 = E(|X - \mu'_1|)$ , and  $\delta_2 = E(|X - M|)$ , respectively. They are dispersion statistics proposed as alternatives to standard deviation. As argued by [Gorard \(2005\)](#), the mean deviations are more efficient in real-life situations where the data contain tiny errors and non-Gaussian distributions. The mean deviations about the mean and the median can be expressed as

$$\delta_1 = 2\mu'_1 F(\mu'_1) - 2m_1(\mu'_1) \quad \text{and} \quad \delta_2 = \mu'_1 - 2m_1(M),$$

respectively, where  $\mu'_1 = E(X)$ ,  $M = \text{Median}(X) = Q(0.5)$  is the median,  $F(\mu'_1)$  is easily determined from (5) and  $m_1(y) = \int_0^y x f(x) dx$  is the first incomplete moment. We can determine  $m_1(y)$  from the sums for  $m_s(y)$  given in (12) by taking  $s = 1$  or using numerical integration.

Other important applications of the previous results refer to the Bonferroni and Lorenz curves, which are central instruments for studying income distribution and inequality analysis. For a given probability  $p$ , they are defined by

$$B(p) = \frac{m_1 [Q(p)]}{p \mu'_1} \quad \text{and} \quad L(p) = \frac{m_1 [Q(p)]}{\mu'_1}$$

respectively, where  $m_1(\cdot)$  follows from (12) and  $Q(\cdot)$  from (10). The Lorenz curve informs about the cumulative proportion of income held by the bottom  $p$  percent of the population, offering a complete picture of the concentration in the distribution (Gómez-Déniz et al., 2022). Figure 5 reports plots for the Bonferroni and Lorenz curves obtained from the WNH distribution, which illustrates the flexibility of the new model to accommodate different inequality patterns.

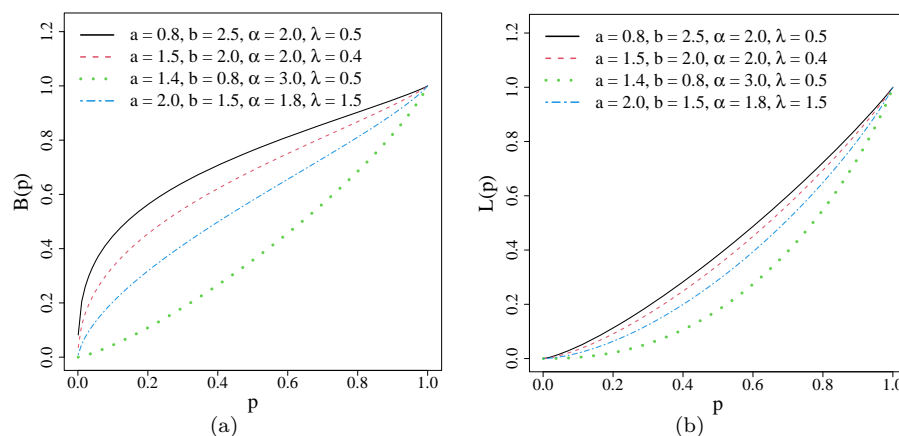


FIGURE 5: Bonferroni and Lorenz curves for some selected scenarios.

## 5. Estimation

Several approaches to parameter estimation for models have been proposed in the literature. However, two, in particular, stand out: maximum likelihood estimation and Bayesian methods. The maximum likelihood estimates (MLEs) have desirable properties that can be used to construct confidence intervals. Additionally, large sample theory for these estimations offers simple approximations for finite samples. On the other hand, Bayesian methods allow the incorporation of prior information in estimation procedures, making them an important alternative when limited data is available or when models are complex and cannot be easily fit with classical methods. This section focuses on estimating the parameter vector  $\boldsymbol{\theta} = (a, b, \alpha, \lambda)$ , which indexes the model WNH using maximum likelihood and the Bayesian approach.

### 5.1. Maximum Likelihood Estimation

Initially, we consider the maximum likelihood method for estimating the unknown parameters of the WNH distribution. Let  $\mathbf{x} = (x_1, \dots, x_n)^\top$  be an observed random sample from the  $WNH(a, b, \alpha, \lambda)$  distribution given by (6). Based on this sample, the log-likelihood function for the parameter vector  $\boldsymbol{\theta} = (a, b, \alpha, \lambda)$  has the form

$$\begin{aligned} \ell(\boldsymbol{\theta}|\mathbf{x}) = & n \log(ab\alpha\lambda) + b \sum_{i=1}^n (1 + \lambda x_i)^\alpha + (\alpha - 1) \sum_{i=1}^n \log(1 + \lambda x_i) - nb \\ & + (b - 1) \sum_{i=1}^n \log\left[1 - e^{1 - (1 + \lambda x_i)^\alpha}\right] - a \sum_{i=1}^n \left[e^{(1 + \lambda x_i)^\alpha - 1} - 1\right]^b. \end{aligned} \tag{13}$$

Equation (13) can be maximized either directly by using the R (`optim` function), SAS (`PROC NLMIXED`) or Ox program (`MaxBFGS` sub-routine) or by solving the non-linear likelihood equations obtained by differentiating (13).

We perform a numerical experiment to illustrate the behavior of Equation (13) and compare it with the log-likelihood in the baseline model. To this aim, we generate a WNH random sample with size  $n = 100$  and  $\boldsymbol{\theta} = (2.7, 5.7, 0.5, 1.0)^\top$  and compute the log-likelihoods corresponding to the WNH and NH distributions by varying the baseline’s parameter values. Figure 6 provides the results of this experiment. Note that the WNH log-likelihood has a higher maximum value for the selected parameter sets and corresponds to the actual value of the generated sample.

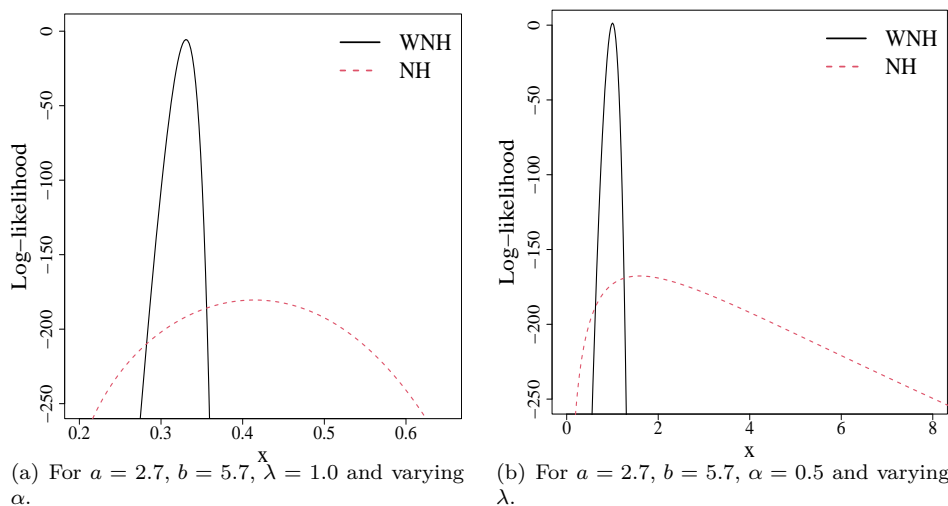


FIGURE 6: Log-likelihood for the WNH and NH distributions computed from WNH random sample with size  $n = 100$  and  $\boldsymbol{\theta} = (2.7, 5.7, 0.5, 1.0)^\top$ .

The components of the score vector  $\mathbf{U}(\boldsymbol{\theta}) = [U_a(\boldsymbol{\theta}), U_b(\boldsymbol{\theta}), U_\alpha(\boldsymbol{\theta}), U_\lambda(\boldsymbol{\theta})]^\top$  can be expressed as

$$\begin{aligned}
 U_a(\boldsymbol{\theta}) &= \frac{n}{a} - \sum_{i=1}^n \left[ e^{(1+\lambda x_i)^\alpha - 1} - 1 \right]^b, \\
 U_b(\boldsymbol{\theta}) &= \frac{n}{b} + \sum_{i=1}^n (1 + \lambda x_i)^\alpha + \sum_{i=1}^n \log \left[ 1 - e^{1-(1+\lambda x_i)^\alpha} \right] \\
 &\quad - a \sum_{i=1}^n \left[ e^{(1+\lambda x_i)^\alpha - 1} - 1 \right]^b \log \left[ e^{(1+\lambda x_i)^\alpha - 1} - 1 \right] - n, \\
 U_\alpha(\boldsymbol{\theta}) &= \frac{n}{\alpha} + b \sum_{i=1}^n (1 + \lambda x_i)^\alpha \log[(1 + \lambda x_i)^\alpha] + \sum_{i=1}^n \log(1 + \lambda x_i) \\
 &\quad + (b-1) \sum_{i=1}^n \frac{(1 + \lambda x_i)^\alpha \log(1 + \lambda x_i) e^{1-(1+\lambda x_i)^\alpha}}{1 - e^{1-(1+\lambda x_i)^\alpha}} \\
 &\quad - a b \sum_{i=1}^n (1 + \lambda x_i)^\alpha \log(1 + \lambda x_i) e^{(1+\lambda x_i)^\alpha - 1} \left[ e^{(1+\lambda x_i)^\alpha - 1} - 1 \right]^{b-1}
 \end{aligned}$$

and

$$\begin{aligned}
 U_\lambda(\boldsymbol{\theta}) &= \frac{n}{\lambda} + (\alpha - 1) \sum_{i=1}^n x_i (1 + \lambda x_i)^{-1} - b \alpha \sum_{i=1}^n x_i (1 + \lambda x_i)^{\alpha-1} \\
 &\quad - a b \alpha \sum_{i=1}^n x_i (1 + \lambda x_i)^{\alpha-1} e^{(1+\lambda x_i)^\alpha - 1} \left[ e^{(1+\lambda x_i)^\alpha - 1} - 1 \right]^{b-1} \\
 &\quad + \alpha (b-1) \sum_{i=1}^n \frac{x_i (1 + \lambda x_i)^{\alpha-1} e^{1-(1+\lambda x_i)^\alpha}}{1 - e^{1-(1+\lambda x_i)^\alpha}}.
 \end{aligned}$$

The MLE  $\hat{\boldsymbol{\theta}}$  of  $\boldsymbol{\theta}$  can also be obtained by setting  $U_a(\boldsymbol{\theta})$ ,  $U_b(\boldsymbol{\theta})$ ,  $U_\alpha(\boldsymbol{\theta})$  and  $U_\lambda(\boldsymbol{\theta})$  equal to zero and solving these equations simultaneously. Once they cannot be solved analytically, we may use iterative techniques such as Newton-Raphson algorithm for the maximization.

The MLEs of all members of the Weibull-G family can be determined from the profile log-likelihood function (Guerra et al., 2021). Thus, taking  $U_a(\boldsymbol{\theta}) = 0$ , we have that a semi-closed MLE for  $a$  is given by

$$\hat{a}(b, \alpha, \lambda) = \frac{n}{\sum_{i=1}^n \left[ e^{(1+\lambda x_i)^\alpha - 1} - 1 \right]^b}.$$

Letting  $\boldsymbol{\theta}_p = (b, \alpha, \lambda)$  and replacing  $\hat{a}$  in (13), we can use the profile log-likelihood to obtain the MLEs for the other three parameters. It is given by

$$\begin{aligned} \ell(\boldsymbol{\theta}_p) &= n \log \left( \frac{n b \alpha \lambda}{\sum_{i=1}^n [e^{(1+\lambda x_i)^\alpha} - 1]^b} \right) + b \sum_{i=1}^n (1 + \lambda x_i)^\alpha \\ &+ (\alpha - 1) \sum_{i=1}^n \log(1 + \lambda x_i) + (b - 1) \sum_{i=1}^n \log [1 - e^{1 - (1 + \lambda x_i)^\alpha}] - n(b + 1). \end{aligned} \tag{14}$$

The maximization of (14) may be simpler than of (13) because it involves only three parameters.

The MLEs have interesting asymptotic properties that allow to construct approximate confidence intervals and testing hypotheses for the model parameters. For  $n$  large, and under standard regularity conditions, the distribution of  $(\hat{a} - a, \hat{b} - b, \hat{\alpha} - \alpha, \hat{\lambda} - \lambda)$  can be approximated by a multivariate normal distribution  $N_4(0, \mathbf{J}(\hat{\boldsymbol{\theta}})^{-1})$ , where  $\mathbf{J}(\hat{\boldsymbol{\theta}}) = -\partial \ell(\boldsymbol{\theta}) / \partial \boldsymbol{\theta} \partial \boldsymbol{\theta}^\top |_{\boldsymbol{\theta} = \hat{\boldsymbol{\theta}}}$  is the observed information matrix. Thus, large-sample-based confidence intervals can be constructed for  $\boldsymbol{\theta}$  using  $\hat{\boldsymbol{\theta}}$ . For the  $100(1 - \eta)\%$  confidence level, these intervals are given by

$$\hat{\boldsymbol{\theta}} \pm z_{\eta/2} \times \left[ \widehat{\text{var}}(\hat{\boldsymbol{\theta}}) \right]^{1/2},$$

where  $z_{\eta/2}$  is the quantile  $\eta/2$  of the standard normal distribution, and  $\widehat{\text{var}}(\hat{\boldsymbol{\theta}}) = \text{diag} \left\{ \mathbf{J}(\hat{\boldsymbol{\theta}})^{-1} \right\}$ .

### 5.2. Bayesian Inference

We also obtain Bayesian estimators for the WNH parameters using Markov Chain Monte Carlo (MCMC) methods due to the complexity of the joint likelihood function. Given an observed random sample  $\mathbf{x} = (x_1, \dots, x_n)^\top$  from the  $\text{WNH}(a, b, \alpha, \lambda)$  distribution, the likelihood function is

$$\begin{aligned} L(\boldsymbol{\theta}|\mathbf{x}) &\propto (a b \alpha \lambda)^n \prod_{i=1}^n (1 + \lambda x_i)^{\alpha-1} \prod_{i=1}^n [1 - \exp\{1 - (1 + \lambda x_i)^\alpha\}]^{b-1} \\ &\times \exp \left\{ -b \sum_{i=1}^n [1 - (1 + \lambda x_i)^\alpha] - a \sum_{i=1}^n [\exp\{(1 + \lambda x_i)^\alpha - 1\} - 1]^b \right\}. \end{aligned}$$

In this case, the Bayesian estimation is constructed under the hypothesis that the unknown parameters are independent and follow a gamma distribution, i.e.,  $\theta_i \sim \text{Gamma}(p_i, q_i)$ ,  $\theta_i \in \boldsymbol{\theta}$ ,  $i = 1, \dots, 4$ , where the hyper-parameters  $(p_i, q_i) > 0$  are known. Thus, the joint prior of parameters  $a, b, \alpha$  and  $\lambda$  is  $p(a, b, \alpha, \lambda) \propto a^{p_1-1} b^{p_2-1} \alpha^{p_3-1} \lambda^{p_4-1} e^{-(q_1 a + q_2 b + q_3 \alpha + q_4 \lambda)}$ . Hence, using Bayes' theorem, the joint

posterior pdf is

$$\begin{aligned} \pi(\boldsymbol{\theta}|\mathbf{x}) &\propto a^{n+p_1-1} b^{n+p_2-1} \alpha^{n+p_3-1} \lambda^{n+p_4-1} \exp\{-(q_1 a + q_2 b + q_3 \alpha + q_4 \lambda)\} \\ &\times \exp\left\{-b \sum_{i=1}^n [1 - (1 + \lambda x_i)^\alpha] - a \sum_{i=1}^n [\exp\{(1 + \lambda x_i)^\alpha - 1\} - 1]^b\right\} \\ &\times \prod_{i=1}^n (1 + \lambda x_i)^{\alpha-1} \prod_{i=1}^n [1 - \exp\{1 - (1 + \lambda x_i)^\alpha\}]^{b-1}. \end{aligned} \quad (15)$$

To obtain the marginal posterior distribution for each parameter in the vector  $\boldsymbol{\theta}$ , we need to integrate Equation (15). However, since the joint posterior distribution is intractable, we use the MCMC approach to draw posterior samples, from which we can infer the marginal distributions. In order to generate samples, we first need to derive the full conditional posterior distributions of the unknown WNH parameters. They can be derived as

$$\pi(a|b, \alpha, \lambda, \mathbf{x}) \propto a^n \exp\left\{-a \sum_{i=1}^n [\exp\{(1 + \lambda x_i)^\alpha - 1\} - 1]^b\right\}, \quad (16)$$

$$\begin{aligned} \pi(b|a, \alpha, \lambda, \mathbf{x}) &\propto \exp\left\{-b \sum_{i=1}^n [1 - (1 + \lambda x_i)^\alpha] - a \sum_{i=1}^n [\exp\{(1 + \lambda x_i)^\alpha - 1\} - 1]^b\right\} \\ &\times b^n \prod_{i=1}^n [1 - \exp\{1 - (1 + \lambda x_i)^\alpha\}]^b, \end{aligned} \quad (17)$$

$$\begin{aligned} \pi(\alpha|a, b, \lambda, \mathbf{x}) &\propto \exp\left\{b \sum_{i=1}^n (1 + \lambda x_i)^\alpha - a \sum_{i=1}^n [\exp\{(1 + \lambda x_i)^\alpha - 1\} - 1]^b\right\} \\ &\times \alpha^n \prod_{i=1}^n (1 + \lambda x_i)^{\alpha-1} \prod_{i=1}^n [1 - \exp\{1 - (1 + \lambda x_i)^\alpha\}]^{b-1}, \end{aligned} \quad (18)$$

and

$$\begin{aligned} \pi(\lambda|a, b, \alpha, \mathbf{x}) &\propto \exp\left\{b \sum_{i=1}^n (1 + \lambda x_i)^\alpha - a \sum_{i=1}^n [\exp\{(1 + \lambda x_i)^\alpha - 1\} - 1]^b\right\} \\ &\times \lambda^n \prod_{i=1}^n (1 + \lambda x_i)^{\alpha-1} \prod_{i=1}^n [1 - \exp\{1 - (1 + \lambda x_i)^\alpha\}]^{b-1}. \end{aligned} \quad (19)$$

Equations (16)-(19) demonstrate that the full conditional distributions of  $a$ ,  $b$ ,  $\alpha$ , and  $\lambda$  can not be expressed as any familiar density function. Then, generating  $\boldsymbol{\theta}$  directly from  $p(a|\cdot)$ ,  $p(b|\cdot)$ ,  $p(\alpha|\cdot)$ , and  $p(\lambda|\cdot)$  is not possible using standard methods. To obtain Bayes estimates for the unknown parameters, we use the Metropolis-Hastings (M-H) algorithm (Metropolis et al., 1953; Hastings, 1970) with a normal proposal distribution. We follow the MCMC sampling procedure outlined below:



Step 1. Choose start values for the parameter vector  $\boldsymbol{\theta} = (a, b, \alpha, \lambda)$ , say  $\boldsymbol{\theta}^{(0)} = (a^{(0)}, b^{(0)}, \alpha^{(0)}, \lambda^{(0)})$ .

Step 2. Set the iteration counter  $j = 1$ .

Step 3. Propose a new value for the  $\boldsymbol{\theta}$  such as  $\boldsymbol{\theta}^* = (a^*, b^*, \alpha^*, \lambda^*)^\top$  by sampling from the proposal distribution:  $\theta_i^* \sim N(\hat{\theta}_i, \hat{J}_{i,i})$ , where  $\theta_i^* \in \boldsymbol{\theta}^*$  and  $i = 1, \dots, 4$ . Here,  $\hat{J}_{i,i}$  is the  $i$ th element of the main diagonal of the observed Fisher information matrix  $\mathbf{J}(\hat{\boldsymbol{\theta}})$ .

Step 4. Calculate the acceptance probability as

$$h(\boldsymbol{\theta}_i^{(j-1)}, \boldsymbol{\theta}_i^*) = \min \left\{ 1, \frac{\pi(\boldsymbol{\theta}_i^* | \boldsymbol{\theta}_{-i}^{(j-1)}, \mathbf{x})}{\pi(\boldsymbol{\theta}_i^{(j-1)} | \boldsymbol{\theta}_{-i}^{(j-1)}, \mathbf{x})} \right\}, \quad i = 1, \dots, 4,$$

where  $\boldsymbol{\theta}_{-i}^{(\cdot)}$  denotes the vector  $\boldsymbol{\theta}^{(\cdot)}$  with its  $i$ th element removed, and  $\pi(\cdot)$  are given in Equations (16)-(19).

Step 5. Generate  $u_i$  ( $i = 1, \dots, 4$ ) from the uniform  $U(0, 1)$  distribution, and if  $u_i < h(\boldsymbol{\theta}_i^{(j-1)}, \boldsymbol{\theta}_i^*)$ , set  $\theta_i^{(j)} = \theta_i^*$ ; otherwise, set  $\theta_i^{(j)} = \theta_i^{(j-1)}$ .

Step 6. Increase the counter from  $j$  to  $j + 1$ .

Step 7. If  $j < M$ , where  $M$  is a large number where convergence is achieved, return to step 3; otherwise, discard the first  $N < M$  samples as burn-in and compute the Bayes estimates as

$$\tilde{\theta}_i = \frac{1}{M - N} \sum_{j=N+1}^M \theta_i^{(j)}.$$

## 6. Simulation Study

In this section, we perform a simulation study to evaluate the performance of the MLE method for the WNH distribution. The study is conducted by computing 10,000 Monte Carlo replications with sample sizes  $n \in \{20, 40, 60, 100, 300, 500\}$ . We use the set of estimates of the parameters obtained in each replication to calculate the mean and root mean squared errors (RMSEs). The data are generated using the inverse transformation method, where  $X = Q(U)$  is obtained from Equation (10). We use Nelder-Mead algorithm to maximize Equation (13) and the observed information matrix is obtained numerically from the optim function in R programming language. Intending to assess the interval estimation, the coverage probability of 95% point-wise confidence interval is computed.

We aim to provide scenarios similar to the observed in a real data set. Hence, we set  $\alpha = 0.1$  and  $\lambda = 1.0$  based on estimated values of the WNH model from the failures times of a Boeing 720 air conditioning system (Proschan, 1963) and

vary  $a$  and  $b$  according to the values reported in Table 2. This table also reports the simulation results. We can verify that, for the selected scenarios, the coverage probabilities are quite close to the nominal level regardless the sample size. The experiment also reveal that the RMSEs of the point estimates decay when the sample size increases. Moreover, the average estimates of the parameters tend to be closer to the true parameter values when  $n$  increases. These results are expected under first-order asymptotic theory.

## 7. Applications

In this section, two applications to real survival data are presented. In order to illustrate the potentiality of the new distribution, we compare the WNH model with nine other related distributions in terms of model fitting. We fit the Kumaraswamy Nadarajah-Haghighi (KwNH) (Vedovatto et al., 2016), GNH, WExp, PGW, exponentiated Weibull (EW) (Mudholkar & Srivastava, 1993), ENH, NH, Weibull, and Gompertz distributions. Their densities are presented in the Appendix A.

The first data set refers to the times of successive failures of the air conditioning system of a fleet with 213 Boeing 720 jet airplanes (Proschan, 1963). The second data set consists of the service times of 63 Aircraft Windshield (Murthy et al., 2004). The unit of measurement is 1000 h. The R codes of all the numerical experiments and applications are available at <https://github.com/penaramirez/WNH>.

Table 3 presents the descriptive statistics for both data sets. For the two samples, the mean is larger than the median and the mode is outlier. The Boeing 720 data have great variance and amplitude, showing more variability than the Aircraft Windshield. The first data set presents positive kurtosis, while the second data set has negative one. Moreover, both data sets present positive skewness, indicating right-skewed data. Note that the WNH model allows fitting skewed data, as explained in Sections 2 and 3.

Tables 4 and 5 list the MLEs (and the corresponding standard errors in parentheses) of the unknown parameters for all fitted models to the first and second data sets, respectively. The Bayes estimates following the procedure described in Section 5.2 are also included. In this case, we run the M-H sampler to generate a Markov chain with 12,000 observations and discard the first 2,000 values as 'burn-in'. These results are obtained using the `AdequacyModel` script in R software (Marinho et al., 2019). We use the simulated-annealing algorithm for maximizing the log-likelihood function for these models.

TABLE 2: Simulation results for a 95% nominal level and  $\alpha = 0.1, \lambda = 1.0$ .

Scenario	n	Mean estimates			RMSEs			Coverage rate					
		$\hat{a}$	$\hat{b}$	$\hat{\lambda}$	$\hat{a}$	$\hat{b}$	$\hat{\lambda}$	$\hat{a}$	$\hat{b}$	$\hat{\lambda}$			
6.5	20	6.14	3.23	0.10	1.61	2.26	0.46	0.01	1.34	99.10	99.94	100.00	99.79
	40	6.12	3.20	0.10	1.61	2.03	0.36	0.01	1.14	98.91	99.99	100.00	99.59
	60	6.13	3.19	0.10	1.58	2.00	0.33	0.01	1.06	98.64	99.96	100.00	99.65
	100	6.20	3.18	0.10	1.53	1.78	0.31	0.01	0.94	98.54	100.00	99.99	99.45
	300	6.52	3.14	0.10	1.38	1.71	0.27	0.01	0.71	97.79	99.99	100.00	99.09
3.0	20	6.68	3.12	0.10	1.32	1.72	0.26	0.01	0.66	97.83	100.00	100.00	99.24
	40	2.88	7.17	0.11	0.99	0.97	1.19	0.02	0.40	99.71	99.32	100.00	99.21
	60	2.94	6.95	0.10	1.10	0.57	0.83	0.01	0.29	99.60	99.73	100.00	99.89
	100	2.97	6.89	0.10	1.14	0.53	0.70	0.01	0.25	99.57	99.84	100.00	99.98
	300	3.01	6.84	0.10	1.17	0.41	0.57	0.00	0.23	99.67	99.88	100.00	100.00
1.5	20	3.06	6.79	0.10	1.21	0.20	0.39	0.00	0.22	99.96	100.00	100.00	100.00
	40	3.08	6.78	0.10	1.22	0.19	0.35	0.00	0.22	100.00	99.97	100.00	100.00
	60	1.53	7.07	0.11	0.96	0.63	1.13	0.02	0.44	99.49	99.14	100.00	98.81
	100	1.49	6.92	0.10	1.10	0.44	0.84	0.01	0.32	99.39	99.55	99.99	99.85
	300	1.51	6.89	0.10	1.15	0.42	0.73	0.01	0.27	99.34	99.67	100.00	99.96
5.7	20	1.53	6.85	0.10	1.18	0.35	0.60	0.00	0.25	99.50	99.83	99.99	100.00
	40	1.55	6.80	0.10	1.22	0.18	0.41	0.00	0.23	99.92	99.68	100.00	100.00
	60	1.55	6.78	0.10	1.23	0.16	0.36	0.00	0.24	99.92	99.41	100.00	100.00
	100	4.80	2.98	0.10	2.04	2.34	0.53	0.02	1.98	96.05	99.54	100.00	99.84
	300	4.77	2.98	0.10	2.01	2.22	0.44	0.02	1.64	96.30	99.64	99.96	99.62
2.7	20	4.78	2.98	0.10	2.00	2.17	0.41	0.01	1.51	96.56	99.89	99.98	99.48
	40	4.85	2.97	0.10	1.94	2.00	0.38	0.01	1.35	96.23	99.92	99.98	99.36
	60	5.09	2.94	0.10	1.76	1.77	0.33	0.01	1.09	94.67	100.00	100.00	98.74
	100	5.27	2.91	0.10	1.64	1.55	0.31	0.01	0.96	94.99	100.00	100.00	98.83
	300	5.27	2.91	0.10	1.64	1.55	0.31	0.01	0.96	94.99	100.00	100.00	98.83

TABLE 3: Descriptive statistics.

Statistics	Real data sets	
	Boeing 720	Aircraft Windshield
Mean	93.14	2.09
Median	57.00	2.06
Mode	14.00	2.50
Variance	11398.47	1.55
Skewness	2.11	0.44
Kurtosis	4.92	-0.27
Minimum	1.00	0.05
Maximum	603.00	5.14
$n$	213	63

We consider the following goodness-of-fit statistics to select the most appropriate model: the Kolmogorov-Smirnov (KS) statistic and the Anderson-Darling ( $A^*$ ) and Cramér-von Mises ( $W^*$ ) corrected statistics. The statistics  $A^*$  and  $W^*$  are based on the empirical cdf, and to obtain them, we can proceed as follows: (i) compute  $\eta_i = F(x_i, \theta)$  where  $F$  is a cdf with known form,  $\theta$  is a  $k$ -dimensional unknown parameter vector and the  $x_i$ 's are in ascending order; (ii) compute  $y_i = \Phi^{-1}(\eta_i)$ , where  $\Phi(\cdot)$  is the standard normal cdf and  $\Phi(\cdot)^{-1}$  its qf; (iii) compute  $u_i = \Phi\{(y_i - \bar{y})/s_y\}$ , where  $\bar{y} = n^{-1} \sum_{i=1}^n y_i$  and  $s_y^2 = (n-1)^{-1} \sum_{i=1}^n (y_i - \bar{y})^2$ ; (iv) calculate  $W^2 = \sum_{i=1}^n \{u_i - (2i-1)/(2n)\}^2 + 1/(12n)$  and  $A^2 = -n - n^{-1} \sum_{i=1}^n \{(2i-1) \log(u_i) + (2n+1-2i) \log(1-u_i)\}$  and (v) modify  $W^2$  into  $W^*(1+0.5/n)$  and  $A^2$  into  $A^* = A^2(1+0.75/n+2.25/n^2)$ . The lower are them, the better is the model adjustment to the data.

Tables 4 and 5 provide the goodness-of-fit statistics for all fitted models to the Boeing 720 and the Aircraft Windshield data sets, respectively. The Bayes estimates for the WNH model give the lowest values of  $A^*$ ,  $W^*$ , and KS for both data sets. So, it could be chosen as the best model among the other known lifetime models, including the generated distributions from the NH baseline model.

Figure 7 displays the histogram and the plots of estimated densities of the three more competitive models according to the goodness-of-fit statistics, whereas the plots of estimated cdfs for these models are displayed in Figure 8. The plots confirm that the WNH distribution yields an effective alternative to other NH generated distributions, such as the KwNH and ENH models in the first application. It also can be useful against other widely known lifetime models, such as the EW and Gompertz models in the second data set. This superiority over its competing models allows unbiased estimators to be obtained for the WNH distribution and, consequently, more appropriate statistical inference, including hypothesis tests, confidence intervals, and prediction intervals. Particularly in engineering, proper fitting of the WNH distribution produces unbiased estimates of important quantities such as hrf, mean residual life, and mean downtime, among others. This can improve preventive maintenance policies. For more details on these latter reliability measures, we refer readers to [Kayid & Izadkhah \(2014\)](#).

TABLE 4: MLEs and goodness-of-fit statistics for the Boeing 720 jet airplanes data set.

Distributions	Estimates				W*	A*	KS
W <sub>NH</sub> ( $a, b, \alpha, \lambda$ )	5.6708 (2.4485)	2.6781 (0.2825)	0.0793 (0.0083)	0.9853 (0.4853)	<b>0.0284</b>	<b>0.2226</b>	<b>0.0323</b>
W <sub>NH</sub> ( $a, b, \alpha, \lambda$ )*	9.0142 (6.8545)	3.0077 (0.3417)	0.0724 (0.0078)	2.0886 (1.3906)	0.0429	0.2951	0.2121
K <sub>wNH</sub> ( $a, b, \alpha, \lambda$ )	1.5797 (0.3358)	0.2124 (0.0891)	0.7244 (0.0793)	0.1344 (0.0517)	0.0311	0.2285	0.0337
G <sub>NH</sub> ( $a, \alpha, \lambda$ )	1.3541 (0.2213)	0.5726 (0.0775)	0.0440 (0.0217)		0.0367	0.2672	0.0373
W <sub>Exp</sub> ( $a, b, \lambda$ )	2.1559 (0.2971)	0.7478 (0.0402)	0.0030 (0.0003)		0.2913	1.7808	0.0954
P <sub>GW</sub> ( $\alpha, \lambda, \gamma$ )	1.5918 (0.1918)	0.2756 (0.0466)	14.8971 (2.534)		0.0827	0.5692	0.0850
E <sub>W</sub> ( $\alpha, \beta, \lambda$ )	0.0279 (0.0111)	0.6187 (0.0883)	2.2841 (0.6961)		0.0411	0.2926	0.0389
E <sub>NH</sub> ( $\alpha, \beta, \lambda$ )	0.5402 (0.0633)	0.0431 (0.0152)	1.3862 (0.2059)		0.0335	0.2534	0.0336
N <sub>H</sub> ( $\alpha, \lambda$ )	0.7256 (0.0891)	0.0188 (0.0044)			0.0782	0.5091	0.0466
Weibull( $\alpha, \lambda$ )	51.9386 (4.2992)	0.7593 (0.0429)			0.1046	0.6634	0.1775
Gompertz( $\theta, \lambda$ )	0.0147 (0.0035)	0.0021 (0.0009)			0.4733	2.8589	0.1397

\*Bayesian estimates

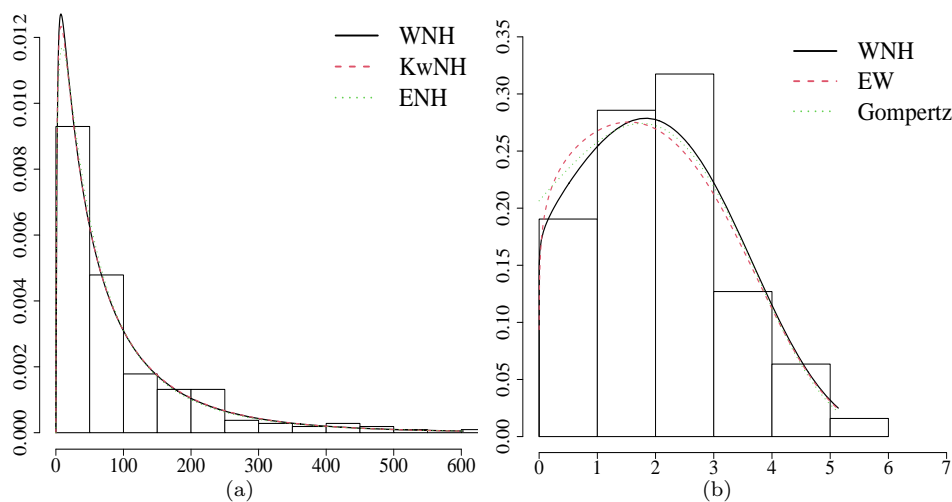


FIGURE 7: Histogram and estimated densities of the (a) W<sub>NH</sub>, K<sub>wNH</sub> and E<sub>NH</sub> models for the Boeing 720 data set; (b) W<sub>NH</sub>, E<sub>W</sub> and Gompertz models for the Aircraft Windshield data set

TABLE 5: MLEs and goodness-of-fit statistics for the Aircraft Windshield data set.

Distributions	Estimates				W*	A*	KS
W $NH(a, b, \alpha, \lambda)$	0.2135 (0.0881)	1.0479 (0.2106)	0.6657 (0.1176)	1.3431 (0.4799)	<b>0.0425</b>	<b>0.2812</b>	<b>0.0628</b>
N $H(a, b, \alpha, \lambda)^*$	0.4066 (0.2896)	1.1104 (0.2628)	0.7359 (0.2544)	1.4010 (1.1326)	0.0899	0.6463	0.4374
K $wNH(a, b, \alpha, \lambda)$	1.2302 (0.3722)	0.2046 (0.0941)	2.6044 (0.4623)	0.4097 (0.1126)	0.0651	0.3975	0.0799
G $NH(a \alpha \lambda)$	1.38304 (0.1867)	4.5360 (1.7030)	0.0916 (0.0412)		0.0697	0.4247	0.0926
W $Exp(a, b, \lambda)$	2.2251 (1.0921)	1.3864 (0.1460)	0.1815 (0.0474)		0.0639	0.3907	0.0698
P $GW(\alpha, \lambda, \gamma)$	1.311 (0.1753)	4.251 (4.5984)	8.979 (9.2221)		0.0576	0.3561	0.0877
E $W(\alpha, \beta, \lambda)$	0.2829 (0.0373)	3.3454 (1.0606)	0.3407 (0.1439)		0.0503	0.3237	0.0739
E $NH(\alpha, \beta, \lambda)$	5.19228 (1.7410)	0.07274 (0.0278)	1.42357 (0.2221)		0.0763	0.4633	0.0939
N $H(\alpha, \lambda)$	6.08583 (2.4754)	0.05458 (0.0242)			0.0754	0.4574	0.1518
Weibull( $\alpha, \lambda$ )	2.308 (0.1869)	1.625 (0.1680)			0.1046	0.6339	0.1095
Gompertz( $\theta, \lambda$ )	0.2065 (0.0498)	0.4882 (0.0984)			0.0449	0.3019	0.0675

\*Bayesian estimates

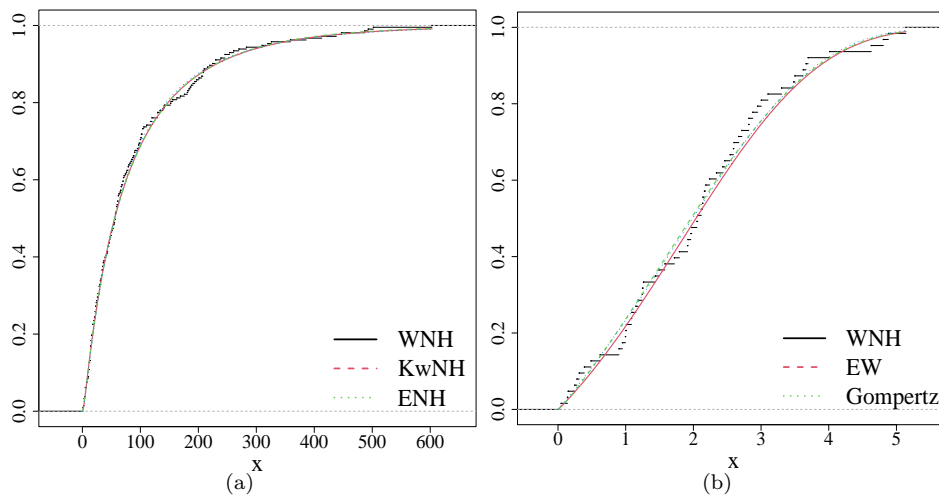


FIGURE 8: Estimated and empirical cdfs of the (a) W $NH$ , K $wNH$  and E $NH$  models for the Boeing 720 data set; (b) W $NH$ , E $W$  and Gompertz models for the Aircraft Windshield data set

## 8. Conclusions

In this paper we introduced a new four-parameter Nadarajah-Haghighi generalization, which may be useful for lifetime applications. More specifically, the introduced model is called *Weibull Nadarajah-Haghighi* (WNH) distribution and is obtained by inserting the Nadarajah-Haghighi model in the *Weibull-G* family (Bourguignon et al., 2014). The proposed distribution allows for greater flexibility of the density function than the Nadarajah-Haghighi density and presents constant, increasing, decreasing, bathtub and upsidedown-bathtub hazard rate shapes. It has the Weibull exponential and Gompertz distributions as sub-models. Some structural properties of the WNH distribution are discussed and the parameter estimation is carried out by maximum likelihood. We also perform a simulation study. In the empirical applications, the WNH distribution is shown quite competitive not only with other NH generated distributions but also to other widely known lifetime models.

[Received: June 2022 — Accepted: May 2023]

## References

- Almarashi, A. M., Algarni, A., Okasha, H. & Nassar, M. (2022), ‘On reliability estimation of Nadarajah-Haghighi distribution under adaptive type-I progressive hybrid censoring scheme’, *Quality and Reliability Engineering International* **38**, 817–833.
- Bagdonavicius, V. & Nikulin, M. (2002), *Accelerated life models: modeling and statistical analysis*, Chapman and Hall/CRC, Boca Raton.
- Bourguignon, M., Lima, M. d. C. S., Leão, J., Nascimento, A. D. C., Pinho, L. G. B. & Cordeiro, G. M. (2015), ‘A new generalized gamma distribution with applications’, *American Journal of Mathematical and Management Sciences* **34**, 309–342.
- Bourguignon, M., Silva, R. B. & Cordeiro, G. M. (2014), ‘The Weibull-G family of probability distributions’, *Journal of Data Science* **12**, 53–68.
- Elshahhat, A., Alotaibi, R. & Nassar, M. (2022), ‘Inferences for Nadarajah-Haghighi parameters via type-II adaptive progressive hybrid censoring with applications’, *Mathematics* **10**, 3775.
- Gómez-Déniz, E., Sarabia, J. M. & Jordá, V. (2022), ‘Parametric Lorenz curves based on the beta system of distributions’, *Communications in Statistics-Theory and Methods* **51**, 8371–8390.
- Gorard, S. (2005), ‘Revisiting a 90-year-old debate: the advantages of the mean deviation’, *British Journal of Educational Studies* **53**, 417–430.

- Guerra, R. R., Peña-Ramírez, F. A. & Cordeiro, G. M. (2021), 'The Weibull Burr XII distribution in lifetime and income analysis', *Anais da Academia Brasileira de Ciências* **93**, e20190961.
- Hastings, W. K. (1970), 'Monte carlo sampling methods using markov chains and their applications'.
- Jiang, R., Ji, P. & Xiao, X. (2003), 'Aging property of unimodal failure rate models', *Reliability Engineering & System Safety* **79**, 113–116.
- Kayid, M. & Izadkhah, S. (2014), 'Mean inactivity time function, associated orderings, and classes of life distributions', *IEEE Transactions on Reliability* **63**, 593–602.
- Kenney, J. & Keeping, E. (1962), *Mathematics of Statistics*, 3 edn, Chapman and Hall Ltda, New Jersey.
- Klutke, G.-A., Kiessler, P. C. & Wortman, M. A. (2003), 'A critical look at the bathtub curve', *IEEE Transactions on reliability* **52**, 125–129.
- Lemonte, A. J. (2013), 'A new exponential-type distribution with constant, decreasing, increasing, upside-down bathtub and bathtub-shaped failure rate function', *Computational Statistics and Data Analysis* **62**, 149–170.
- Louzada, F., Ramos, P. L. & Nascimento, D. (2018), 'The inverse Nakagami-m distribution: A novel approach in reliability', *IEEE Transactions on Reliability* **67**, 1030–1042.
- Marinho, P. R. D., Cordeiro, G. M., Ramírez, F. P., Alizadeh, M. & Bourguignon, M. (2018), 'The exponentiated logarithmic generated family of distributions and the evaluation of the confidence intervals by percentile bootstrap', *Brazilian Journal of Probability and Statistics* **32**, 281–308.
- Marinho, P. R. D., Silva, R. B., Bourguignon, M., Cordeiro, G. M. & Nadarajah, S. (2019), 'Adequacy model: An r package for probability distributions and general purpose optimization', *PloS One* **14**, e0221487.
- Martínez-Flórez, G., Pacheco-López, M. & Tovar-Falón, R. (2022), 'Likelihood-based inference for the asymmetric exponentiated bimodal normal model', *Revista Colombiana de Estadística* **45**, 301–326.
- Metropolis, N., Rosenbluth, A. W., Rosenbluth, M. N., Teller, A. H. & Teller, E. (1953), 'Equation of state calculations by fast computing machines', *The journal of chemical physics* **21**, 1087–1092.
- Moors, J. (1988), 'A quantile alternative for kurtosis', *The statistician* **88**, 25–32.
- Mudholkar, G. & Srivastava, D. (1993), 'Exponentiated Weibull family for analyzing bathtub failure-rate data', *IEEE Transactions on Reliability* **42**, 299–302.
- Murthy, D., Xie, M. & R, J. (2004), *Weibull models*, Wiley, New York.



- Nadarajah, S. & Haghighi, F. (2011), 'An extension of the exponential distribution', *Statistics* **45**, 543–558.
- Oguntunde, P., Balogun, O., Okagbue, H. & Bishop, S. (2015), 'The Weibull-exponential distribution: Its properties and applications', *Journal of Applied Sciences* **15**, 1305–1311.
- Oluyede, B. & Liyanage, G. W. (2023), 'The gamma odd Weibull generalized-g family of distributions: Properties and applications', *Revista Colombiana de Estadística* **46**, 1–44.
- Peña-Ramírez, F. A., Guerra, R. R., Canterle, D. R. & Cordeiro, G. M. (2020), 'The logistic Nadarajah-Haghighi distribution and its associated regression model for reliability applications', *Reliability Engineering & System Safety* **204**, 107196.
- Peña-Ramírez, F. A., Guerra, R. R. & Cordeiro, G. M. (2019), 'The Nadarajah-Haghighi Lindley distribution', *Anais da Academia Brasileira de Ciências* **91**, e20170856.
- Peña-Ramírez, F. A., Guerra, R. R., Cordeiro, G. M. & Marinho, P. R. (2018), 'The exponentiated power generalized Weibull: Properties and applications', *Anais da Academia Brasileira de Ciências* **90**, 2553–2577.
- Pérez, J. M. P., Márquez, F. P. G., Tobias, A. & Papaelias, M. (2013), 'Wind turbine reliability analysis', *Renewable and Sustainable Energy Reviews* **23**, 463–472.
- Peter, P. O., Oluyede, B., Bindele, H. F., Ndwapi, N. & Mabikwa, O. (2021), 'The gamma odd burr iii-g family of distributions: Model, properties and applications', *Revista Colombiana de Estadística* **44**, 331368.
- Proschan, F. (1963), 'Theoretical explanation of observed decreasing failure rate', *Technometrics* **5**, 375–383.
- Ramos, P. L., Nascimento, D. C., Cocolo, C., Nicola, M. J., Alonso, C., Ribeiro, L. G., Ennes, A. & Louzada, F. (2018), 'Reliability-centered maintenance: Analyzing failure in harvest sugarcane machine using some generalizations of the Weibull distribution', *Modelling and Simulation in Engineering* **2018**, 1241856.
- Silva, G. O., Ortega, E. M. & Cordeiro, G. M. (2010), 'The beta modified Weibull distribution', *Lifetime Data Analysis* **16**, 409–430.
- Silva, R., Gomes-Silva, F., Ramos, M., Cordeiro, G. M., Marinho, P. & Andrade, T. (2019), 'The exponentiated Kumaraswamy-G class: General properties and application', *Revista Colombiana de Estadística* **42**, 133.
- Singla, N., Jain, K. & Sharma, S. K. (2012), 'The beta generalized Weibull distribution: properties and applications', *Reliability Engineering & System Safety* **102**, 5–15.

Tahir, M., Cordeiro, G. M., Mansoor, M., Zubair, M. & Alizadeh, M. (2016), ‘The Weibull-Dagum distribution: Properties and applications’, *Communications in Statistics-Theory and Methods* **45**.

Tahir, M. H. & Nadarajah, S. (2015), ‘Parameter induction in continuous univariate distributions: Well-established G families’, *Anais da Academia Brasileira de Ciências* **87**, 539–568.

VedoVatto, T., Nascimento, A. D. C., Miranda Filho, W. R., Lima, M. C. S., Pinho, L. G. & Cordeiro, G. M. (2016), ‘Some computational and theoretical aspects of the exponentiated generalized Nadarajah-Haghighi distribution’, *arxiv.org/abs/1610.08876v1*.

Xu, M., Drogue, E., Lins, I. & Moura, M. D. C. (2017), ‘On the q-Weibull distribution for reliability applications: an adaptive hybrid artificial bee colony algorithm for parameter estimation’, *Reliability Engineering & System Safety* **158**, 93–105.

## Appendix A. Alternative distributions fitted in the applications

This appendix presents the distributions fitted in section 7 as competitive models to the Weibull Nadarajah-Haghighi distribution. These models and their corresponding densities are listed below (for  $x > 0$ ):

- The KwNH density (VedoVatto et al., 2016) is given by

$$f(x) = a b \alpha \lambda \frac{(1 + \lambda x)^{\alpha-1} [e^{1-(1+\lambda x)^\alpha}]^\alpha \left\{ 1 - [e^{1-(1+\lambda x)^\alpha}]^\alpha \right\}^{a-1}}{\left\{ 1 - [1 - e^{1-(1+\lambda x)^\alpha}]^\alpha \right\}^{1-b}}.$$

- The GNH density (Bourguignon et al., 2015) is given by

$$f(x) = \frac{\alpha \lambda}{\Gamma(a)} (1 + \lambda x)^{\alpha-1} [(1 + \lambda x)^\alpha - 1]^{a-1} e^{1-(1+\lambda x)^\alpha}.$$

- The WExp density (Oguntunde et al., 2015) is given by

$$f(x) = a b \lambda (1 - e^{\lambda x})^{b-1} e^{-b \lambda x - a(e^{\lambda x} - 1)^b},$$

and it is a particular case of the proposed model when  $\alpha = 1$ .

- The PGW density (Bagdonavicius & Nikulin, 2002) is given by

$$f(x) = \alpha \lambda \gamma (1 + \lambda x^\gamma)^{\alpha-1} e^{1-(1+\lambda x^\gamma)^\alpha}.$$

- The EW density (Mudholkar & Srivastava, 1993) is given by

$$f(x) = \alpha \beta \lambda x^{\alpha-1} \exp(-\lambda x^\alpha) [1 - \exp(-\lambda x^\alpha)]^{\beta-1}.$$

- The ENH density (Lemonte, 2013) is given by

$$f(x) = \alpha \beta \lambda \frac{(1 + \lambda x)^{\alpha-1} \exp\{1 - (1 + \lambda x)^\alpha\}}{[1 - \exp\{1 - (1 + \lambda x)^\alpha\}]^{1-\beta}}.$$

- The NH density given by (4).
- The Weibull density is given by

$$f(x) = \alpha \lambda (\lambda x)^{\alpha-1} e^{-(\lambda x)^\alpha}.$$

- The Gompertz density is given by

$$f(x) = \theta e^{\lambda x} e^{\frac{\theta}{\lambda} (e^{\lambda x} - 1)},$$

and it a particular case of the proposed model when  $\alpha = \beta = 1$ .

The parameters of the above densities are all positive real numbers.